Bulk Properties of a Cyanogel Network: Toward an Understanding of the Elastic, Mechanical, and Physical Processes Associated with Sol−Gel Processing of Cyanide-Bridged Gel Systems

Stefanie L. Sharp and Andrew B. Bocarsly*

Department of Chemistry, Princeton University, Princeton, New Jersey 08544-1009

George W. Scherer*

Department of Civil Engineering and Operations Research, Princeton University, Princeton, New Jersey 08544-1009

Received August 18, 1997. Revised Manuscript Received November 24, 1997

The reaction of aqueous solutions of Na_2PdCl_4 and $K_3Co(CN)_6$ results in gelatinous polymeric materials, characterized by bridging cyanides between the central metals of the adducts. Such materials are referred to as cyanogels. A mechanical perturbation method, three-point beam-bending, was used to measure the viscoelastic relaxation behavior and permeability of a series of Pd/Co cyanogels of differing concentrations. The shear and Young's modulii of the cyanogel network was found to increase with an increase in concentration. Permeability was found to decrease with an increase in concentration, and was found to range from 239 to 3.67 nm^2 over the concentration range 0.175−0.600 M. This suggests that the Pd/Co cyanogel contains an average pore structure size with the radii ranging from 40 to 5 nm over the concentration range investigated.

Introduction

Solution sol−gel processing, the formation of a gel from a reaction involving molecular precursors followed by the removal of solvent, has become a ceramic processing technique for the formation of oxide-based ceramics.[1] Via sol−gel processing, one has the ability to control and predict the properties of the bulk product by manipulating the molecular properties of the precursors. To implement such a synthetic strategy, the relationship between the sol properties and the bulk properties of the resulting gel must be understood.[1] For the case of silica-based gels, it has been shown[2] that the mechanical properties and permeabilities of the gel can be obtained from a simple three-point bending experiment. When a gel beam is deflected in a three-point bending experiment, two types of relaxation processes occur. The first, hydrodynamic relaxation, is caused by the flow of liquid within the gel network, and the second, viscoelastic relaxation, is related to the polymer network itself. The total relaxation is found to be approximately equal to the product of the hydrodynamic and viscoelastic relaxation functions.[2] By immersing a beam of an aqueous gel in a water bath, bending it to a constant deflection, and measuring the load on the gel as a function of time, it is possible to determine the permeability, as well as the elastic modulus and Poisson's ratio of the gel network.[3] The permeability obtained by beam bending has been shown[3] to be the same as that obtained by a previously described thermal expansion method[4] or by direct flow measurements[5] (although the latter method is much more difficult and less accurate). Moreover, the pore size deduced from the permeability (measured by beam bending) agrees well with sizes determined by nitrogen desorption.[6,7]

We have recently reported that aqueous solutions of the square-planar complex K_2PdCl_4 and $K_xM(CN)_n$ [where $n = 4-8$ and M is a transition metal] react to form gelled polymeric materials as indicated by eq 1:[8]

$$2x[PdCl_4]^{2-} + x[M(CN)_6]^{n-} \rightarrow [(CN)_4M(CN)_2-\{\text{trans-}PdCl_2\}_2]_x^{n-} + 4xCl^- \quad (1)$$

The product polymer is characterized by bridging cyanides between the Pd(II) and M metal centers forming a star−polymer system as illustrated by the Pd/Co polymer system in Figure 1.[9] If we consider one Co

* To whom correspondence should be addressed.

(1) Brinker, G. J.; Scherer, G. W. *Sol−Gel Science: The Physics and Chemistry of Sol−Gel Processing*; Academic Press: Boston, MA, 1990.
(2) Scherer, G. W. *J. Sol-Gel Sci. Technol.* **1994**, *1*, 169−175.
(3) Scherer, G. W. *J. Non-Cryst. Solids.* **1992**, *142*, 18−35.
(4) Scherer, G. W.; Hdach, H.; Phalippou, J. *J. Non-Cryst. Solids.* **1991**, *130*, 157−170.
(5) Scherer, G. W.; Swiatek, R. M., *J. Non-Cryst. Solids.* **1989**, *113*, 119−129.
(6) Scherer, G. W. *J. Non-Cryst. Solids*, **1997**, *215*, 155−168.
(7) Scherer, G. W.; Alviso, C.; Pekola, R.; Gross, J. In *Microporous and Macroporous Materials*; Flobo, R., Beck, J. S., Suib, S. L., Corbin, D. R., Davis, M. E., Iton, L. E., Zones, S. I., Eds.; MRS: Pittsburgh, PA, 1996; pp 497−503.
(8) Pfennig, B. W.; Bocarsly, A. B.; Prud'homme, R. K. *J. Am. Chem. Soc.* **1993**, *115*, 2661−2665.

S0897-4756(97)00571-1 CCC: $15.00
Published on Web 02/10/1998

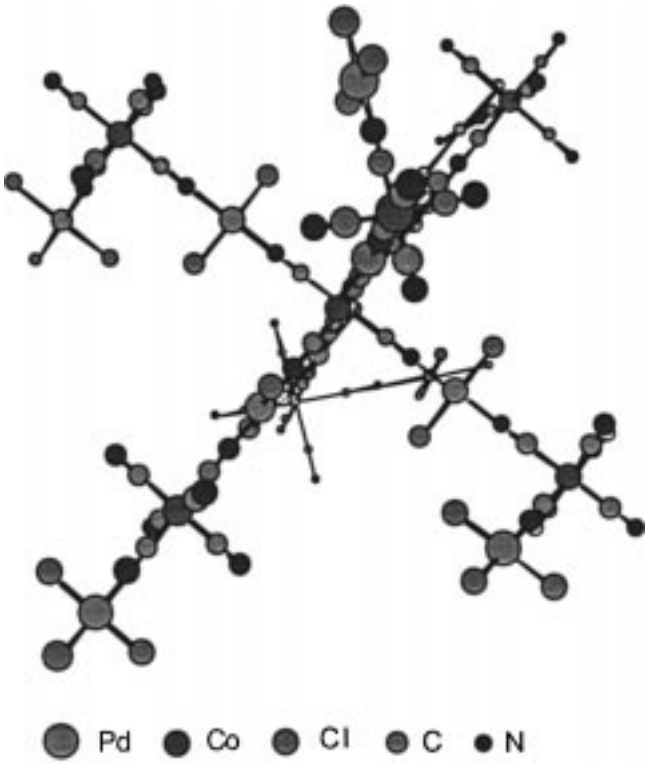

Figure 1. Proposed star polymer structure of cyanogel polymer network.

metal as a center of the star, then six cyanide bridges would be formed. Polymerization occurs via substitution of two chloride ligands, trans to each other, on the Pd(II) centers by the nitrogen end of the cyanide ligand to generate the extended bridging cyanide structure shown in the Figure.[9] Because the bridging cyanide ligand framework is central to these gels and distinguishes them from classic metal−oxo gels, we refer to them as cyanogels.

The thermal chemistry of cyanogels has been shown to exhibit a high degree of synthetic versatility allowing for a variety of well-defined solid-state products ranging from metal alloys to oxide ceramics and semiconductors.[10,11] Here we report on the mechanical properties of the Pd/Co cyanogel; a system that has a well-defined processing chemistry to produce alloy and ceramic products.[11] From the response of the gel to a bending perturbation, we deduce the permeability of the gel, bulk attributes of the gel's pore structure, and the fundamental bulk mechanical constants associated with gel polymer structure.

Experimental Section

To make a series of cyanogel "beams", equimolar aqueous solutions of Na_2PdCl_4 and $K_3Co(CN)_6$ (in concentrations ranging from 0.175 to 0.600 M) were mixed in a 2:1 volume ratio (Na_2PdCl_4 solution to $K_3Co(CN)_6$ solution) and the mixed solution poured into a glass tube (12.5 mm i.d.) mold. Both starting materials were reagent grade, obtained from either Alfa or Aldrich, and were used as received. To make cyanogel beams of concentrations 0.450 M and higher, the solutions were first placed in an ice bath and chilled to 0 °C to prevent premature gelling of the mixed solutions. Gel beam samples were allowed to age for 1 week at 9 °C in the glass mold. During this time a small amount of water was expelled from the beam and the beam diameter decreased ~20% allowing it to be easily removed from the mold. After the aging period, further variation in the physical dimensions of the gel were not noted. Upon removal from the mold, the beams were placed in a deionized water bath at room temperature. The water was changed daily for approximately 4 days to remove excess salts from the gels. When the addition of a 0.5 M silver nitrate solution to the bath no longer formed a precipitate, indicating no free chloride, this treatment was suspended. This process was carried out since excess salt not directly associated with the cyanogel polymer would cause the flow of liquid through the gel beam to be controlled by osmotic properties instead of by the induced mechanical perturbation of the beam. The gel beams produced were generally of 70−80 mm in length and 10−10.5 mm in diameter. Previous work[3] has shown that a length/diameter ratio exceeding ~7 gives purely extensional behavior for a gel in bending.

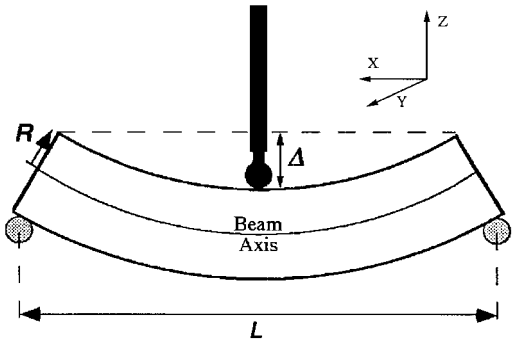

Figure 2. Schematic illustration of three-point bending fixture: Gel beam with radius *R* rests on supports a distance *L* apart while immersed in a bath of water. A deflection Δ is gradually imposed at the midpoint of the bar, and the force exerted by the gel on the pushrod is measured as a function of time.

To carry out the beam bending experiment the gel beams were supported at the ends on Teflon roller supports that prevented the development of axial tension or additional moments in the samples. A container with a capacity of ~750 mL was cut from a block of Teflon, and the end supports were secured to the bottom of the container with stainless steel screws. After the container was filled with deionized water at room temperature, the gel beam was placed onto the end supports, and an aluminum pushrod was brought into contact with the gel at its midpoint as illustrated in Figure 2. The diameters of the supports and pushrod were 6 mm.

The pushrod was lowered onto the gel rod at a constant speed (~0.025 mm/s) to induce a deflection in the cyanogel beam.[3] This method was used, rather than sudden deflection, because some of the gels were so soft that rapid deflection caused inconvenient oscillations in the gel. The total deflection imposed was sufficiently small enough so that the maximum strain in the gel was <1% except in the case of the 0.175 M gel which had a maximum strain of ~2%. A screw driven by an Oriel motorized precision translator (Model 16128, with Model 18008 controller) controlled the pushrod position. The load, $W(t)$, required to sustain the deflection was recorded using a Sensotech load cell (Model 31/1435-01 with Model GM signal conditioner). The beam was generally deflected 0.7−1.7 mm. Data were recorded at a rate of ~8 points/s, digitized, and collected using equipment described previously.[3] Table 1 indicates the experimental samples utilized, providing the number of samples evaluated and the number of recorded deflections per sample. Good reproducibility was obtained from sample to sample at fixed cyanogel concentration. All data were T-tested. Standard error (provided in Table 2) was utilized to monitor the random error.

(9) Heibel, M. Sol−Gel Chemistry of the New Inorganic Polymers−Cyanogels. Ph.D. Thesis, University of Ljubljana, 1996.
(10) Heibel, M.; Kumar, G.; Wyse, C.; Bukovec, P.; Bocarsly, A. B. *Chem. Mater.* **1996**, *8*, 1504−1511.
(11) Bocarsly, A. B.; Kumar, G.; Heibel, M. *Mater. Res. Soc. Symp. Proc.* **1994**, *346*, 89−93.

Table 1. Cyanogel Beam Sample Pool

concn[a] (M)	ρ_b[b] (g/cm^3)	total no. of samples run	no. of runs
0.175	0.0413	1	2
0.225	0.0577	3	5
0.250	0.0673	4	6
0.300	0.0798	3	5
0.350	0.0914	3	5
0.400	0.102	3	5
0.450	0.118	2	4
0.500	0.129	2	4
0.550	0.137	2	4
0.600	0.150	2	3

[a] Concentration of inital solutions used in synthesizing the cyanogel. [b] Bulk density of cyanogel.

Table 2. Fitting Parameters for Eq 16

concn (M)	τ_b[a] (s)	ν[b]	τ_{VE}[c] (s × 1000)	b[d]	standard error[e]
0.175	2950	0.167	11.7	0.8506	0.00099
0.225	1460	0.197	11.8	0.7771	0.00031
0.250	965	0.149	14.2	0.7354	0.00040
0.300	641	0.191	15.3	0.8724	0.0015
0.350	566	0.178	17.5	0.8663	0.0099
0.400	589	0.161	17.6	0.8482	0.0046
0.450	530	0.168	19.9	0.8019	0.0040
0.500	466	0.194	24.7	0.8571	0.0069
0.550	497	0.164	24.1	0.8145	0.0076
0.600	457	0.166	22.4	0.8191	0.0078

[a] Hydrodynamic relaxation time. [b] Poisson's ratio. [c] Viscoelastic relaxation time. [d] Distribution breadth. [e] Standard error of fitted curves.

Bulk density (ρ_b) measurements (see Table 1) of the gel polymer were obtained by measuring the dimensions of the gel beams with Mitutoyo Digimatic calipers. Beams were then dehydrated by drying in an oven at 95 °C, and the mass of the xerogel was determined using a Mettler H31AR balance. Helium pycnometry measurements on the xerogel, to measure the skeletal density (ρ_s) of the polymer network, were performed with a Micromeritics Accupync 1330 helium pycnometer.

Aerogels were made by first exchanging the water within the pores of the gel with acetone. The acetone-impregnated gel beams were then placed in a computer-controlled CO_2-drying autoclave, and the acetone was then exchanged with liquid CO_2. To ensure that all acetone was exchanged, the autoclave was flushed five times with CO_2. The autoclave was brought up to 9 MPa and 45 °C to extract the then supercritical CO_2 from the gel beams. During the extraction process, the gel beam diameter shrank ~20%. Imaging of the aerogels was accomplished with a Philips XL30 FEG scanning electron microscope (SEM).

Theory

Determination of the modulus of a gel requires consideration of the movement of liquid in the pores under an applied load.[4,13] Part of the applied load is supported by the liquid, and part by the solid network, when a gel is deformed. To measure the properties of the solid phase, the load must be sustained until the flow of liquid allows the pressure in the liquid to drop to zero, and the load to be transferred entirely to the solid network. When a fully hydrated gel is deformed, the liquid cannot instantly flow out of the network, so the gel behaves as if it were incompressible. Consider the application of an instantaneous strain imposed on a free-standing gel beam perpendicular to the beam axis (the perpendicular axis is defined as the z axis), the associated movement of the liquid will stretch the network in the x and y directions such that no net change in volume of the gel occurs under the incompressibility assumption. This ratio of the applied stress to the instantaneous strain in the z direction is the shear modulus of the network, G. However, if the strain is sustained long enough, the liquid flows from the network into the bath. This continues until the pressure differential between the liquid in the gel and in the bath goes to zero; then, as in a normal elastic body, the uniaxial stress produces a dialation of the body. The ratio of the stress to the final uniaxial strain yields E, Young's modulus. The time constant for this relaxation depends on the permeability of the network to the flow of liquid in the gel pores.[12]

As illustrated in Figure 2, when the gel beam is deflected by the pushrod, the top portion of the gel is compressed and the bottom portion of the gel is stretched. Consequently, a compressive load is placed on both the liquid phase of the gel and the polymer phase of the gel which is adjacent to the pushrod, while the polymer network and the internal gel liquid are placed in tension below the beam axis. In principle, the elastic modulus of the gel might be different in tension and compression, whereas our analysis assumes that it is the same. Recent work on silica aerogels[14] has shown that the same modulus is obtained in tension and compression, even at strains much larger than those used in our study. In the present study, the sample diameter was sufficently small so that the deformation was pure bending, and the strain was therefore proportional to the deflection. If the deflection is held constant, the internal liquid flows through the polymer network and between the network and the bath until the pressure differential in the internal gel liquid goes to zero, and all of the load is transferred to the solid network polymer of the gel. As the liquid flows, the measured load decreases. The kinetics of load decay can be analyzed to determine the permeability and elastic modulus of the gel;[3] if the gel is viscoelastic, the relaxation function can also be determined.[15] In our experiments, the strain was maintained at a small enough level to assume that the modulus was not affected by the deformation. It has been shown that relaxation of the load proceeds in two steps: first, the flow of the liquid (called hydrodynamic relaxation) reduces the load, typically by ~20%, and then, over a much longer period of time, viscoelastic relaxation of the polymeric gel network allows the load to drop gradually toward zero.[2,11] In the following analysis, we ignore flow of liquid along the axis of the beam, since the utilized beams were much longer than their diameter; thus, virtually all of the flow is normal to the gel beam axis.[3]

The movement of liquid through a porous body, including polymeric gels, has been reported[5,16] to obey Darcy's law,[17] which states that the flux (J) is proportional to the pressure gradient in the liquid:

(12) Scherer, G. W. *J. Sol-Gel Sci. Technol.* **1994**, *1*, 285.
(13) Scherer, G. W. *J. Non-Cryst. Solids* **1989**, *109*, 183−190.
(14) Hafidi, A.; Woignier, W.; Phalippou, J.; Scherer, G. W.; Hiki, A. Comparison Between Flexural and Uniaxial Compression Tests to Measure the Elastic Modulus of Silica Aerogel, manuscript in preparation.
(15) Scherer, G. W. *J. Sol-Gel Sci. Technol.* **1994**, *2*, 199−204.
(16) Tokita, M.; Tanaka, T. *J. Chem. Phys.* **1991**, *95*, 4613−4619.

$$J = -\frac{D}{\eta_L}\nabla p \tag{2}$$

where η_L is the viscosity of the pore liquid and D is the permeability (which has units of area). By analogy to Poiseuille's law for flow through a pipe, D is predicted to be proportional to the porosity (ϕ) of the body and the square of the mean pore size (r):

$$D = \phi r^2/4\kappa \tag{3}$$

where κ is a constant that accounts for the tortuosity of the pores. Porosity can also be defined as $1 - \rho$, where ρ is the relative density ($\rho = \rho_b/\rho_s$). Since the pores in the network are expected to be small, even though the porosity is typically high, the permeability of a gel is expected to be extremely low. An equivalent way to understand the permeability of a gel is to recognize that resistance to flow results from friction between the network and the liquid, and the huge interfacial area of the gel creates enormous friction.

Biot developed a theory to describe the response of a porous, partially saturated medium to applied loads.[18−20] For an isotropic gel in which the solid network is linearly elastic, Biot showed that the axial strain (ϵ_x) could be written in terms of the principal total stresses (σ_x, σ_y, σ_z) as[21]

$$\epsilon_x = \frac{1}{E}[\sigma_x - \nu(\sigma_y + \sigma_z)] + \frac{(1 - 2\nu)P}{E} \tag{4}$$

where P is the stress in the liquid (equal to the pressure, but opposite in sign). The quantities E and ν represent the properties that one would measure if the liquid were drained from the pores; ν is Poisson's ratio for the network, and E is Young's modulus. The total stresses represent the sum of forces on the liquid and solid phases on a cross section divided by the area of the section.[22]

Sudden deflection of very soft gels, such as those under study here, in three-point bending can cause oscillations that confound the measurement of stress relaxation. The oscillations can be avoided by using a constant deflection rate, rather than a sudden deflection; then the permeability and elastic properties of the gel can be obtained by analyzing the applied force as a function of time. This problem was solved previously for the case of a gel with an elastic network.[3,23] When the solid network is viscoelastic, the most convenient method for solving a problem of this kind is to use the Laplace transform with respect to time, t:[24]

$$\tilde{f}(x, s) \equiv \int_0^\infty \exp(-st) f(x, t)\, dt \tag{5}$$

If a stress analysis has been done for an elastic material, then the viscoelastic analogy states that the corresponding solution for a viscoelastic material can be found directly from the elastic solution.[25] This is done by replacing the elastic stresses, strains, and moduli in the elastic equations with the Laplace transforms of the corresponding viscoelastic quantities, and then inverting the transform. This approach was used in ref 2 to determine the relaxation behavior of a viscoelastic gel subjected to a sudden fixed deflection. An important assumption made is that the Poisson's ratio of the network does not relax. The rationale for this assumption is that Poisson's ratio (ν) depends on the structure of the network, rather than the properties of the solid; therefore, even if the Poisson's ratio of the solid phase changes from ~0.2 (characteristic of the elastic solid) to 0.5 (characteristic of a liquid) as the gel relaxes, ν of the network will remain the same, as long as the architecture of the network is not significantly altered. In this case, the transform of Young's modulus is written as

$$\tilde{E} = E\tilde{\psi}_{VE} \tag{6}$$

where ψ_{VE} is the viscoelastic relaxation function and E is the instantaneous Young's modulus of the gel network.

In the following, we adapt the solution from ref 2 to the case of a gel subjected to a certain rate of deflection, $\dot{\Delta}$. The starting point for this analysis is eq 17 of ref 2:

$$s\tilde{\epsilon} = -\frac{D}{\eta_L}\nabla^2\tilde{P} \tag{7}$$

where ϵ is the volumetric strain of the network. This equation simply states that the rate of contraction of the gel in any local region is equal to the net flux of the liquid out of that region. Using the form of the Laplacian operator appropriate for cylindrical coordinates, eq 7 becomes

$$\frac{1}{u}\frac{\partial}{\partial u}\left(u\frac{\partial P}{\partial u}\right) + \frac{1}{u^2}\frac{\partial^2 P}{\partial \phi^2} = -\left(\frac{\eta_L a^2}{D}\right)\frac{\partial \epsilon}{\partial t} \tag{8}$$

where r and ϕ are cylindrical coordinates, a is the radius of the gel rod, and $u = r/a$. The strain rate is given by eq 6 of ref 23:

$$\frac{\partial \epsilon}{\partial t} = -\frac{24(1 - 2\nu) r \sin(\phi) z}{L^3}\frac{\partial \Delta}{\partial t} - \frac{1 - 2\nu}{G}\frac{\partial P}{\partial t} \tag{9}$$

where z is the axial coordinate, L is the distance between supports under the bar of gel, and G is the instantaneous shear modulus. The Laplace transform of eq 9 is

$$s\tilde{\epsilon} = -\left(\frac{24(1 - 2\nu) a z s\tilde{\Delta}}{L^3}\right) u \sin(\phi) - \frac{2(1 + \nu)(1 - 2\nu) s\tilde{P}}{s\tilde{E}} \tag{10}$$

so the transform of eq 8 becomes

$$\frac{1}{u}\frac{\partial}{\partial u}\left(u\frac{\partial \tilde{P}}{\partial u}\right) + \frac{1}{u^2}\frac{\partial^2 \tilde{P}}{\partial \phi^2} - c_1\tilde{P} = c_2 u \sin\phi \tag{11}$$

(17) Happel, T.; Brenner, H. *Low Reynolds Number Hydrodynamics*; Martinus Nijhoff: Dordrecht, 1983.
(18) Biot, M. A. *J. Appl. Phys.* **1941**, *12*, 155−164.
(19) Biot, M. A. *J. Appl. Phys.* **1954**, *25*, 1385−1391.
(20) Biot, M. A. *J. Appl. Phys.* **1962**, *33*, 1482−1498.
(21) Scherer, G. W. *Langmuir* **1996**, *12*, 1109−1116.
(22) Scherer, G. W. *J. Non-Cryst. Solids* **1989**, *109*, 171−182.
(23) Scherer, G. W. *J. Non-Cryst. Solids* **1996**, *201*, 1−25.
(24) Hildebrand, F. B. *Methods of Applied Mathematics*, 2nd ed.; Prentice Hall: Englewood Cliffs, NJ, 1962.
(25) Scherer, G. W. *Relaxation in Glass and Composites*; Wiley: New York, 1986; Krieger: Malabar, FL, 1992.

where

$$c_1 \equiv \left(\frac{\eta_L a^2}{D}\right)\frac{2(1+\nu)(1-2\nu)}{\tilde{E}}$$

$$c_2 \equiv \left(\frac{\eta_L a^2}{D}\right)\left(\frac{24az(1-2\nu)}{L^3}\right)s\tilde{\Delta} \qquad (12a,b)$$

The formal solution to eq 11 is

$$\tilde{P} = \left(\frac{24azG}{L^3}\right)\left(\frac{\sin\phi}{\tau_b}\right)\sum_{n=1}^{\infty}\frac{2J_1(B_n u)}{B_n J_0(B_n)}\left(\frac{s\tilde{\Delta}}{1/\tilde{\psi}_{VE} + B_n^2/\tau_b}\right) \qquad (13)$$

where J_0 and J_1 are Bessel functions of the first kind of order 0 and 1, respectively, and B_n is a root of J_1, $J_1(B_n) = 0$. The hydrodynamic relaxation time (τ_b), the characteristic time for fluid flow within the gel beam, is defined by

$$\tau_b = \frac{(1-2\nu)\eta_L a^2}{DG} \qquad (14)$$

The transform of the force, W, exerted on the gel by the pushrod to maintain a displacement of Δ is given by eq 15 of ref 2:

$$\tilde{W} = \frac{48\Delta I\tilde{E}}{L^3} - \frac{2(1-2\nu)}{z}\int_0^a\int_0^{2\pi}\tilde{P}r^2\sin\phi\,dr\,d\phi \qquad (15)$$

where I is the moment of inertia of the gel rod; for a cylinder of radius a, $I = \pi a^4/4$. Inserting eq 13 into eq 15 and inverting the transform leads to

$$W(t) = \frac{144GI}{L^3}\int_0^t \Omega(t-t')\frac{\partial\Delta}{\partial t'}\,dt' \qquad (16)$$

where

$$\Omega(t) = \frac{2(1+\nu)}{3}\psi_{VE}(t) + \frac{8(1-2\nu)}{3}\sum_{n=1}^{\infty}\frac{g_n(t)}{B_n^2} \qquad (17)$$

and

$$g_n(t) \equiv \frac{1}{1/\tilde{\psi}_{VE} + B_n^2/\tau} \qquad (18)$$

It was shown in ref 2 that eq 17 is represented quite accurately by

$$\Omega(t) \approx R(t)\psi_{VE}(t) \qquad (19)$$

where R is a function describing the hydrodynamic relaxation of a gel rod with an elastic network

$$R(t) = \frac{2(1+\nu)}{3} + \frac{8(1-2\nu)}{3}\sum_{n=1}^{\infty}\frac{\exp(-B_n^2 t/\tau_b)}{B_n^2} \qquad (20)$$

and ψ_{VE} is the viscoelastic relaxation function which describes the kinetics of uniaxial stress relaxation under constant strain. The value ψ_{VE} cannot be calculated from first principles;[21] for the purposes of fitting the data, it is convenient to use a stretched exponential function, which has been shown to fit a wide variety of relaxation processes:[25]

$$\psi_{VE}(t) = \exp[-(t/\tau_{VE})^b] \qquad (21)$$

where b is a constant ($0 \le b \le 1$) and τ_{VE} is the viscoelastic relaxation time. Thus, the load on the viscoelastic gel can be found by evaluating eq 16 with Ω given by eq 19. The fitting parameters are τ_b, ν, b, and τ_{VE}.

The pushrod and end supports dent the gel significantly,[23] so eq 16 should be modified by replacing Δ with $\Delta - \delta$, where δ is the depth of the indentation:

$$W(t) = \frac{144GI}{L^3}\int_0^t \Omega(t-t')\frac{\partial(\Delta-\delta)}{\partial t'}\,dt' \qquad (22)$$

The indentation depth can be calculated from eq 59 of ref 21 (with c_0 in eq 59 replaced by c from eq 67 of that paper).[26]

From the initial load on and deflection of the gel beam, the shear modulus (G), the ratio of shear stress to strain, can be calculated; then Young's modulus, E, is computed using G

$$E = 2(1+\nu)G \qquad (23)$$

With the fitted value of ν, the longitudinal modulus can also be determined. The fitted value of τ_b from eq 20 can be used with eq 14 to calculate permeability of the gel.

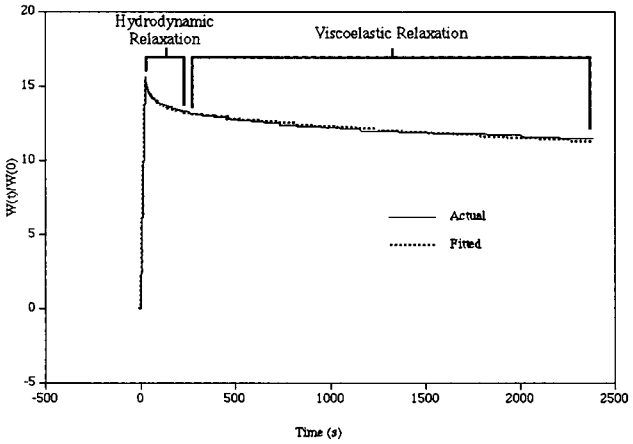

Figure 3. Normalized load on cyanogel beam as a function of time: (a) measured $W(t)/W(0)$ and (b) curve fitted to eq 16. $W(0)$ is the load before the deflection is imposed upon the beam.

Results

A typical relaxation curve, along with the least-squares fit of the data, is shown in Figure 3. The first part of the load decay (extending to ~500 s) results from hydrodynamic relaxation, as liquid flows within the gel, and between the gel and the bath. The subsequent slow relaxation is the viscoelastic response of the cyanogel network to the applied strain. Average fitting parameters for the cyanogel concentrations explored are shown in Table 2. The exponent, b, is constant and close to 1, so the viscoelastic relaxation function is nearly a simple exponential.

The permeability of a gel, a measure of fluid flow through the gel, controls its response to mechanical loads.[1] The permeability (D) was calculated from eq 14

Table 3. Cyanogel Moduli and Permeability

concn (M)	G^a (MPa)	E^b (MPa)	H^c (MPa)	D^d (nm^2)
0.175	0.0630	0.147	0.157	239 ± 11
0.225	0.123	0.291	0.324	164 ± 5.7
0.250	0.286	0.650	0.670	113 ± 4.3
0.300	0.418	0.968	1.07	72.8 ± 3.8
0.350	0.591	1.37	1.53	43.0 ± 2.9
0.400	0.887	2.02	2.14	35.7 ± 2.7
0.450	1.18	2.94	3.57	24.5 ± 2.5
0.500	1.64	3.91	4.30	16.6 ± 2.0
0.550	1.99	4.62	4.97	7.44 ± 1.36
0.600	2.36	5.36	5.66	3.67 ± 1.12

[a] Shear modulus. [b] Young's modulus. [c] Longitudinal modulus. [d] Cyanogel permeability ± one standard deviation unit.

Table 4. Cyanogel Permeability Parameters

concn (M)	$\rho_b/\rho_s{}^a$	$\kappa_\omega{}^b$	$r_\omega{}^c$ (nm)	$V_p{}^d$ (cm^3/g)	η_L/D^e (dyn·s/cm^4)
0.175	0.0183	1.68	40.4 ± 3.7	23.8	3.99×10^9
0.225	0.0255	1.77	34.5 ± 2.6	16.9	3.82×10^9
0.250	0.0297	1.82	29.1 ± 2.2	14.4	8.44×10^9
0.300	0.0352	1.88	23.9 ± 2.2	12.1	1.31×10^{10}
0.350	0.0404	1.92	20.9 ± 2.0	10.5	2.22×10^{10}
0.400	0.0451	1.96	17.1 ± 1.8	9.36	2.67×10^{10}
0.450	0.0522	2.01	14.4 ± 1.9	8.03	3.89×10^{10}
0.500	0.0567	2.04	12.0 ± 1.7	7.31	5.45×10^{10}
0.550	0.0605	2.07	8.09 ± 1.42	6.86	1.28×10^{11}
0.600	0.0662	2.10	5.75 ± 1.40	6.22	2.60×10^{11}

[a] Cyanogel relative density. [b] Kozeny "constant". [c] Mean pore radii ± one standard deviation unit. [d] Pore volume per gram. [e] Hydrodynamic resistance, "friction factor".

using the parameters listed in Table 2, and assuming that the viscosity of the liquid inside the gel was identical with that of bulk water at 22 °C ($\eta_L = 9.54 \times 10^{-4}$ Pa·s)[27] These values are given in Table 3 along with average permeability and moduli data. Helium pycnometry measurements on three different xerogel samples yielded a skeletal density (ρ_s) of the gel of 2.26 ± 0.03 g/cm^3. The relative density of the gels ($\rho = \rho_b/\rho_s$), a measure of how porous the gel framework is, can be determined using the skeletal density and is listed in Table 4.

Discussion

Viscoelastic relaxation in gels is attributed to attack by the pore liquid on the bonds that constitute the network. For example, in silica gels, it has been determined that the viscoelastic effect results from chemical attack (hydrolysis) by water on strained siloxane bonds in the network.[15,28,29] For the cyanogel polymeric network, viscoelasticity presumably occurs due to the metal centers undergoing ligand exchange between the strained bridging cyanide bonds and water, allowing the network to relax. The viscoelastic response time increases with the higher concentration samples because the stress concentration on the load-bearing polymeric network is greater in the lower concentration gels, where there is less of a framework to support the load, than in the higher concentration gels. With the greater strain applied to the lower concentration cyanogel network, the rate of ligand exchange should be higher. It has been demonstrated in recent experiments that chemical attack does occur preferentially on strained siloxane bonds in silica gels.[6] The shape of the viscoelastic relaxation function as reflected in the value of b in the stretched exponential function is invariant within experimental error with the gel density.

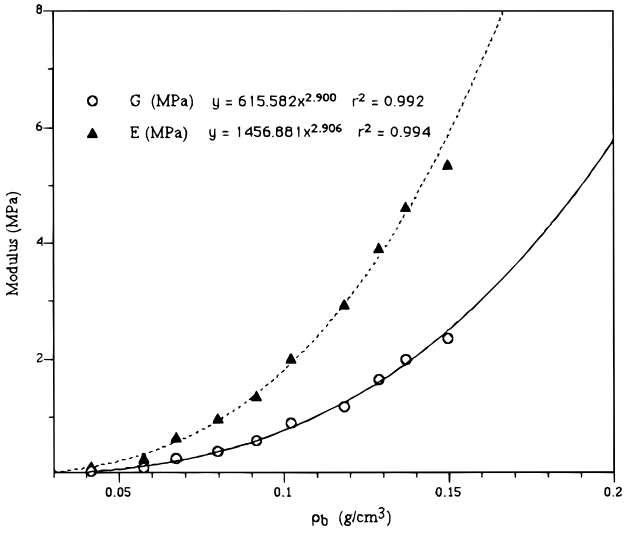

Figure 4. Shear modulus (G) and Young's modulus (E), found from beam-bending experiments, fitted to power-law curve (eq 24).

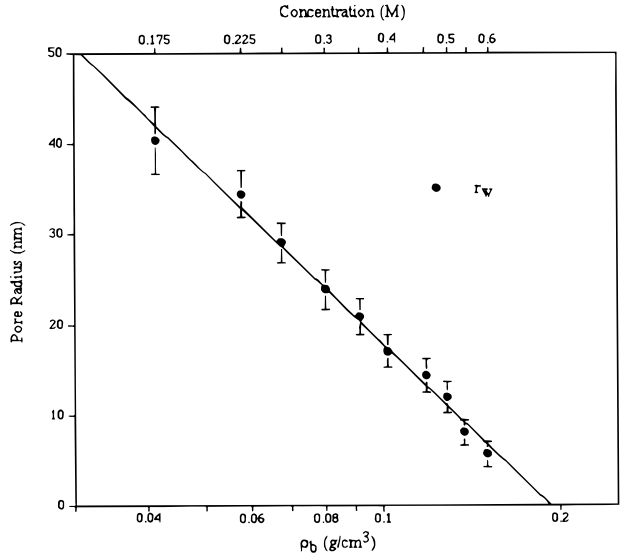

Figure 5. Pore radius, r_ω, calculated using eqs 25 and 20 fitted to a log curve.

Figure 4 shows that shear (G) modulus varies with bulk density (ρ_b) according to a power law:

$$G = G_0(\rho_b/\rho_0)^m \qquad (24)$$

where m is curve fit to a value of 2.9. G_0 and ρ_0 are the values of the shear modulus and bulk density of the samples under normal conditions. Analogous behavior is observed for Young's modulus, as also illustrated in Figure 4. A power-law dependence of modulus on density has been reported to apply to a wide variety of

(26) Software for performing the curve fitting is available from the author.

(27) *CRC Handbook of Chemistry and Physics*, 62 ed.; Weast, R. C., Astle, M. J., Eds.; CRC Press: Boca Raton, FL, 1981; p F-42.

(28) Scherer, G. W. *Faraday Discuss.* **1995**, *101*, 225−234, 287−291.

(29) Sharp, K. G.; Scherer, G. W. *J. Sol-Gel Sci. Technol.* **1997**, *8*, 165−171.

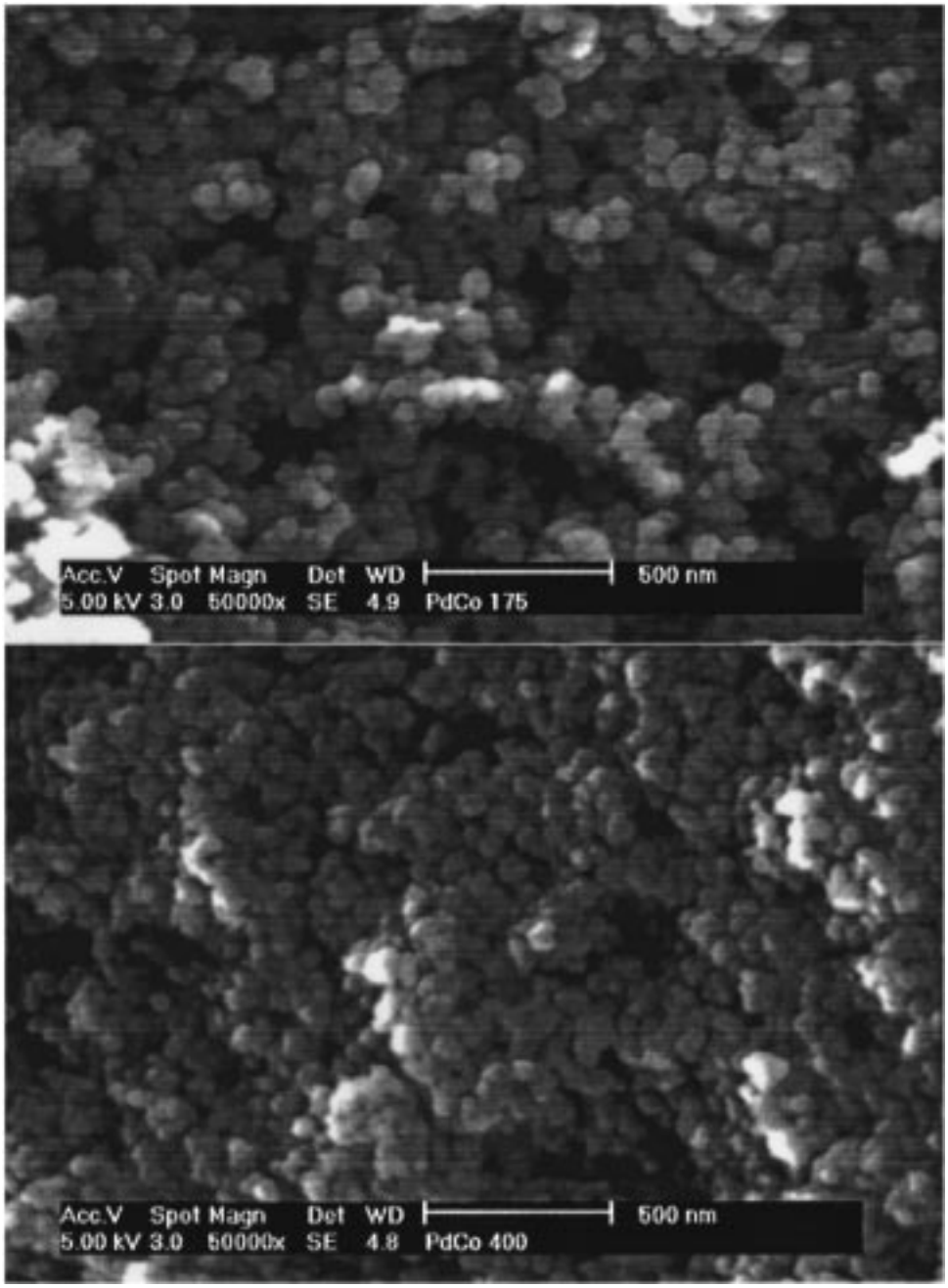

Figure 6. SEM images of the fracture surface of aerogels made from 0.175 M (top) and 0.400 M (bottom) cyanogels. From these images it can be concluded that the pore size measured through the beam bending experiments is comparable to the pore size observed in the images.

gels,[30] but the exponent has been found to vary widely from system to system. The physical basis for the power-law behavior has not been established.

For many materials, the permeability can be related by using the Carman−Kozeny equation to the mean pore size, r_ω.[17] The Carman-Kozeny equation was developed for granular materials, but describes flow through networks as well. It has been reported to be well suited to the calculation of the permeability of fractal networks:[31]

$$r_\omega = \left[\frac{4D\kappa_\omega}{1 - \rho_b/\rho_s}\right]^{1/2} \qquad (25)$$

The value κ_ω is the Kozeny "constant," a weak function of porosity, which is slightly dependent on ρ_b. It is intended to account for the noncircular cross section and nonlinear path of the pores in a real material.[32] For a network consisting of a random array of cylinders, κ_ω is given approximately by[15]

$$\kappa_\omega \approx 1.0 + 6.05\rho^{0.5} - 8.60\rho + 6.58\rho^{1.5} \qquad (26)$$

By using the permeability calculated from eq 14, the mean pore size of the gel can thus be determined using eqs 25 and 26. Contained in Table 4 are the data for permeability parameters and calculated mean pore radii (r_ω). The observed variation of pore size with bulk

(30) Gross, J.; Scherer, G. W.; Alviso, C.; Pekala, R. *J. Non-Cryst. Solids* **1997**, *211*, 132−142.
(31) Adler, P. M. *Phys. Fluids* **1986**, *29*, 15.
(32) Scherer, G. W. *J. Non-Cryst. Solids* **1989**, *113*, 107−118.

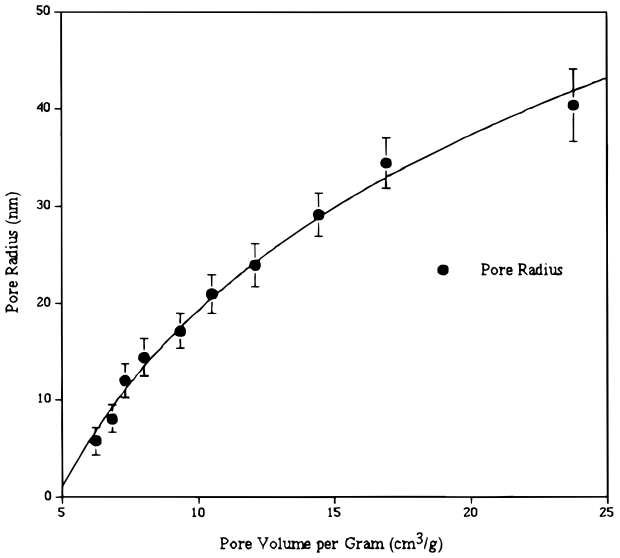

Figure 7. Pore radius (r_ω) versus pore volume per gram (V_p) fitted to a log curve.

density and concentration is illustrated in Figure 5. When aerogels formed from cyanogels are fractured and imaged by SEM (Figure 6), it can be seen that the calculated mean pore radii corresponds to the typical pore radii found in the aerogels. Thus, the available data indicates that the beam bending method is a reliable method of determining the pore size within the cyanogel system.

The low permeability of a gel is due to the friction between the gel network and the liquid within the pores of the gel.[33] This hydrodynamic resistance between the network and the pore liquid is a measurable quantity known as the "friction factor" (η_L/D), and the values for the cyanogel system are listed in Table 4. The values are of the same order of magnitude and are comparable to those of the poly(acrylamide) gel system.[34] As with the poly(acrylamide) gel system, by changing the concentration of the starting solutions by a factor of 2, the friction factor changes by an order of magnitude.

The observed variation between the pore radius and the pore volume per gram (V_p) is plotted in Figure . Pore volume per gram is given by the difference of the inverse gel density and inverse polymer density. In terms of fundamental properties of the gel, r_ω is not directly related to V_p. However, a linear dependence of pore size on pore volume per gram has been found in several studies of silica gel.[35−37] A linear fit of r_ω versus V_p for silica gives an indication of how high the relative density of the silica gel can be before the pores close. In other words, the final density of the gels during drying and processing can be predicted. For the cyanogel system, the dependence of pore size on V_p is logarithmic. If this line is extrapolated to zero, it indicates that the relative density of the dried cyanogel is ~0.084 which is similar to the density of the hydrated cyanogel and an order of magnitude lower than the relative density of the xerogel (0.79). Since a prediction for the densified material should be an order of magnitude higher than the extrapolated value, we conclude that increased cyanogel polymer concentration does not produce a bulk structure which is similar to the structure obtained by dehydrating the hydrogel to form a xerogel.

Conclusions

The technique of three-point beam bending has been successfully applied to the cyanogel system to determine hydrodynamic properties, mechanical parameters, and pore structure. As with silica gels, cyanogels exhibit both hydrodynamic and viscoelastic relaxation. When comparing cyanogels and B2-type silica gels of roughly the same density, some similarities and differences of their physical properties are noticed.[28] The moduli (Young's, shear, and longitudinal) are comparable, indicating that the gels are of comparable "stiffness." Poisson's ratio for the cyanogel system is a little higher (6%) when compared to the B2-type silica gels which is an indication that the cyanogel system is slightly more deformable and that the strengths of the cross-links are a little weaker. Permeability is smaller for cyanogels (3.67 nm^2 vs 21.4 nm^2) than for the silica gels, indicating a finer microstructure.[5] This phenomenon is seen in organic gels, where samples with the same quantity of monomer, but different amounts of cross-linking agent, have drastically different permeabilities.[38] Increased permeability in this case has been associated with inhomogeneously distributed cross-links, creating relatively open regions through which most of the liquid flows. Based on the low permeability of the cyanogels, therefore, it can be concluded that the structure of the cyanogel pore network is fairly uniform. Since the permeability decreases as the density of the cyanogel network is increased, it can also be concluded that as the concentration of the cyanogel is increased, more bridging cyanide bonds are formed.

CM970571Z

(33) Johnson, D. L.; *J. Chem. Phys.* **1982**, *77*, 1531−1539.
(34) Tanaka, T.; Hocker, L. O.; Benedek, G. B. *J. Chem. Phys.* **1973**, *59*, 5151−5159.
(35) Wallace, S.; Brinker, C. J.; Smith, D. M. *Better Ceramics Through Chemistry VI*; Materials Research Society: Pittsburgh, PA, 1995; pp 241−246.
(36) Reichenauer, G.; Stumpf, C.; Fricke, J. *J. Non-Cryst. Solids* **1995**, *186*, 334−341.
(37) Smith, D. M.; Scherer, G. W.; Anderson, J. M. *J. Non-Cryst. Solids* **1995**, *188*, 191−206.
(38) Weiss, N.; van Uliet, T.; Silberberg, A. *J. Polym. Sci.: Polym. Phys. Ed.* **1979**, *17*, 2229−2240.